# ARTICLE

## Intrinsic acetamide brush-off by polyurea biodendrimers

Nuno Martinho,*[a] Rita F. Pires,[a] Mire Zloh[b,c] and Vasco D. B. Bonifácio*[a]

The presence of genotoxic impurities in active pharmaceutical ingredients (APIs) is a major concern in pharmaceutical industry. Acetamide is a common genotoxic byproduct found in many APIs synthetic routes, mainly due to acetonitrile hydrolysis, and selective scavenging is a still a challenging task. Herein, as a proof-of-concept, we evaluate polyurea (PURE) biodendrimers as strategic nanopolymers to prepare safe drug nanoformulations from mixtures containing acetamide, using *(S)*-ibuprofen (IBF) as a model drug. Furthermore, computational molecular dynamics (MD) simulations were conducted to rationalize *in vitro* results and to identify the key intermolecular interactions within mixtures. Experimental data was corroborated by MD simulations which showed that PURE biodendrimers are able to efficently complex drug molecules with a high payload.

## Introduction

A major concern in pharmaceutical industry is the production of active pharmaceutical ingredients (APIs) with a safe profile suitable for clinical use. In this process, both APIs and solvents may lead to the formation of side products with a possible toxicity that could put in risk millions of patients. Therefore, the presence of genotoxic impurities is controlled and must adhere to strict concentration guidelines. However, the removal of such impurities via traditional methods usually lack specificity and requires the extensive use of solvents and sometimes a significant loss of API. Hence, the development of novel APIs purification protocols is a top priority.

Acetamide is a common impurity found in APIs syntheses with a genotoxic potential that requires a rigorous control and removal [1,2]. Recently, we described the use of molecular imprinted polymers (MIPs) as a simple, clean, and sustainable strategy for acetamide removal [3]. We propose now a new purification strategy based on dendrimer polymers. Dendrimers are a class of synthetic branched polymeric materials whose unique architecture and well-defined structure may be suitable to develop selective nanosorbents. Due to the presence of dynamic and accessible internal cavities, dendrimers can act as host macromolecules and encapsulate of guest-molecules into their interior [4–8]. Their unparalleled batch-to-batch reproducibility (in contrast with other polymers) is highly desirable feature. These properties can both be leveraged for controlled release purposes [9], as well as for purification [10,11], and thus be potentially extended to acetamide removal. In this regard, we have previously observed the formation of acetamide as a by-product in the synthesis of polyurea (PURE) biodendrimers, as a result of *N,O*-bis(trimethylsilyl)acetamide (BSA) hydrolysis [12]. In the purification process we often saw that acetamide crystallized out of the dendrimer crude mixture before the dialysis purification step. This observation prompted us to ponder that if PURE biodendrimers interacted poorly with acetamide they could be potential candidates for the purification of APIs containing acetamide as an impurity. Notwithstanding, PURE biodendrimers are also prime polymers for APIs purification purposes since the high content of urea groups facilitate hydrogen bonding and thus confer extra binding selectivity. Furthermore, these nanopolymers display pH-dependent ionization of both terminal (primary) and internal (tertiary) amine groups which can be used for controlled drug loading and release. Finally, such systems are also thermodynamically stable (up to 120 °C, at least [12]) which makes them robust, green nanosorbent systems.

Herein, we investigated the potential of PURE biodendrimers to act as an efficient nanofiltration system by assessing their affinity and selectivity towards complexation of a selected API in aqueous media containing acetamide. Previous computational studies already demonstrated that it is possible to both rationalize and predict the behavior of dendrimers structure and examine the properties that favor interaction with small molecules [13]. Therefore, we applied molecular dynamics (MD) simulations to investigate the interactions of PURE biodendrimers with acetamide and *(S)*-ibuprofen (IBF), a model API. We show that MD simulations corroborate our experimental observations and provide a solid basis for future studies on intermolecular interactions in the systems that contain APIs, dendrimers, and side products. Ultimately, this study will have a strong impact in the preparation of drug nanoformulations that are acetamide-free and safe for the use in therapeutic protocols based on controlled drug delivery.

[a.] Institute for Bioengineering and Biosciences, Instituto Superior Técnico, Universidade de Lisboa, Lisboa, Portugal.
E-mail: nunomartinho@tecnico.ulisboa.pt; vasco.bonifacio@tecnico.ulisboa.pt
[b.] School of Life and Medical Sciences, University of Hertfordshire, Hatfield, United Kingdom.
[c.] Faculty of Pharmacy, University Business Academy, Novi Sad, Serbia.
† Electronic Supplementary Information (ESI) available.
See DOI: 10.1039/x0xx00000x

## Results and discussion

Generation 4 polyurea biodendrimer (PURE$_{G4}$) was obtained as an brownish oil via a previously established green chemistry methodology [12]. During this process it was observed that acetamide crystallized out of the crude oil mixture taken from the polymerization reactor (Fig. S1). This result prompted us to further investigate how PURE biodendrimers interact with acetamide as this behavior differs from other experimental observations suggesting that there is low affinity of PURE biodendrimers towards acetamide. PURE biodendrimers generally display a favorable uptake of small molecules, including IBF, that can be loaded up to 50% w/w [14]. Therefore, leveraging the inability of PURE biodendrimers to uptake acetamide, they could be used as "nanosponges" for selective encapsulation of APIs contaminated by acetamide contamination. This phenomenon would allow combining purification and ultimately developing a nanoformulation for the controlled drug delivery of therapeutics. To evaluate this possibility, IBF was selected as a model API since it is a well-studied low molecular weight molecule that is hydrophobic and practically insoluble in water (21 mgL$^{-1}$, DrugBank record DB01050). Moreover, it contains a carboxyl group whose ionization can be controlled by pH to study its role in PURE dendrimers interactions. The most properties of IBF are in the stark contrast to acetamide.

A physical mixture of PURE$_{G4}$ with acetamide alone at both pH 6 and 9 showed no differences in the $^1$H NMR spectra at concentrations up to 200 equivalents and only at such high concentration it was possible to observe changes when compared to the spectra of PURE$_{G4}$ biodendrimer (Figs. 1A and 1B). However, at 1000 equivalents a new peak at 1.74 ppm and a better separation between 2.59 and 2.45 ppm were observed which likely corresponds to changes of chemical shifts induced by interactions between the terminal amines and acetamide (Fig. 1A).

In contrast, the addition of 37 equivalents (50% w/w) of the water-insoluble IBF resulted in its complete dissolution in deuterated water (otherwise insoluble) and in dramatic changes in both the $^1$H and $^{13}$C NMR of PURE$_{G4}$ at both pH 6 and pH 9 (Figs. 1A, 1B and 1C). At pH 6 the proton changes are only apparent in the region around 3.5 ppm which is characteristic of changes in the environment around the urea groups whereas there are also changes between in the region 2.2-2.8 ppm at pH 9 which indicates internalization of IBF into the interior of PURE$_{G4}$. This may be due to more aggregation between branches at higher pH that may create hydrophobic pockets that favor interactions with IBF. Nevertheless, the results suggest that PURE biodendrimers overall interact poorly with acetamide while can incorporate high payloads of IBF. The nature of the interaction seems to be both electrostatic and *via* hydrogen bonding between the drug and the urea groups, as previously reported.[14]

Dendrimers are remarkable host 3D nanopolymers. They generally allow multiple interactions both in the internal cavities and at the surface, thus enabling a range of interactions and complexation that can interact selectively with a variety of molecules of different sizes. PURE biodendrimers show a very high loading capacity towards IBF, but this property that has been also reported for poly(amidoamine) (PAMAM) dendrimers, where urea groups are substituted by amides [4,5,15,16]. The solubilization effect by dendrimers has been shown to be pH-dependent and both the

hydrogen bonding capacity and the hydrophobic character are determinants of the interactions and the maximum loading.

To further rationalize our results and compare to observations with PAMAM dendrimers, all-atom MD simulations were carried. To mimic the conditions of interest relevant to the *in vitro* results, all-atom models of PURE$_{G4}$ at pH 6 and pH 9 were generated by reported methods [17,18]. and simulated in a water box model. RMSD and $R_g$ were used to determine when dendrimers structure reached equilibrium (Fig. S2, ESI†) and the overall structural properties of these dendrimers was summarized in Table 1. At pH 6 the amine terminal groups are protonated and, consequently, PURE biodendrimers display a more open conformation (higher radius of gyration, $R_g$) and consequently a more spherical shape (higher $\Omega_S$) compared to PURE$_{G4}$ at pH 9. This occurs because, at acidic pH, the protonated terminal amines exert electrostatic repulsion, therefore repelling the dendrimer branches. On the contrary, at basic pH these amine groups are in their neutral state allowing interbranch interactions to occur via hydrogen bonding which leads to backfolding into a more closed conformation [19].

Despite the structural differences between PURE and PAMAM dendrimers (polyurea *vs.* polyamide backbones, respectively), their size ($R_g$) was found to be similar [20,21]. Furthermore, PURE biodendrimers are built from a tridentate core amine (TREN), which leads to a more open conformation. This has implications for loading purposes since the more open conformation also means there is a significant higher water penetration and consequently higher water content close to the center of mass which ultimately results in a less favorable environment for molecules such as IBF. This may explain why IBF loading into PURE$_{G4}$ is lower in PAMAM counterparts.

**Table 1.** Structural characterization of PURE biodendrimers obtained by MD simulations.

| Dendrimer | pH | $M_W$ | Nº. NH$_2$ shell | Nº. Ureas core-shell | $R_g$ (nm) | $\Omega_S$ |
|---|---|---|---|---|---|---|
| PURE$_{G4}$ | 6 | 7985 | 48 | 45 | 2.15±0.05 | 0.75 |
| PURE$_{G4}$ | 9 | 7897 | 48 | 45 | 1.81±0.03 | 0.55 |
| PURE$_{G5}$ | 6 | 16364 | 96 | 93 | 2.57±0.01 | 0.72 |
| PURE$_{G6}$ | 6 | 33070 | 192 | 189 | 2.99±0.13 | 0.82 |

Equilibrated conformations of PURE$_{G4}$ biodendrimers obtained from MD simulations were further simulated in the presence of 20 molecules of either acetamide or IBF that were randomly distributed within a spherical shell around the periphery of the PURE biodendrimer in the water box. In a qualitative agreement with *in vitro* observations, within 5 ns only three acetamide molecules remained near the dendrimer at pH 9, and zero molecules at pH 6 (Fig. 2). This is in stark contrast with simulations using IBF, considering that within the same time scale 12 molecules were found in the proximity of the dendrimer, more specifically near to the dendrimer terminal ends (Fig. 2).

Upon inspection of the last frame of simulation, it could be observed that the dendrimer interacts with the IBF carboxylic acid via electrostatic contacts with the protonated primary amine, as well as by hydrogen bonding with the urea groups (Fig. S3, ESI†), which agrees with reported FT-IR data [20]. The location of the IBF molecules within the dendrimer was mostly found to be distributed at the periphery, as previously found for PAMAM-loaded IBF [22].

# ARTICLE
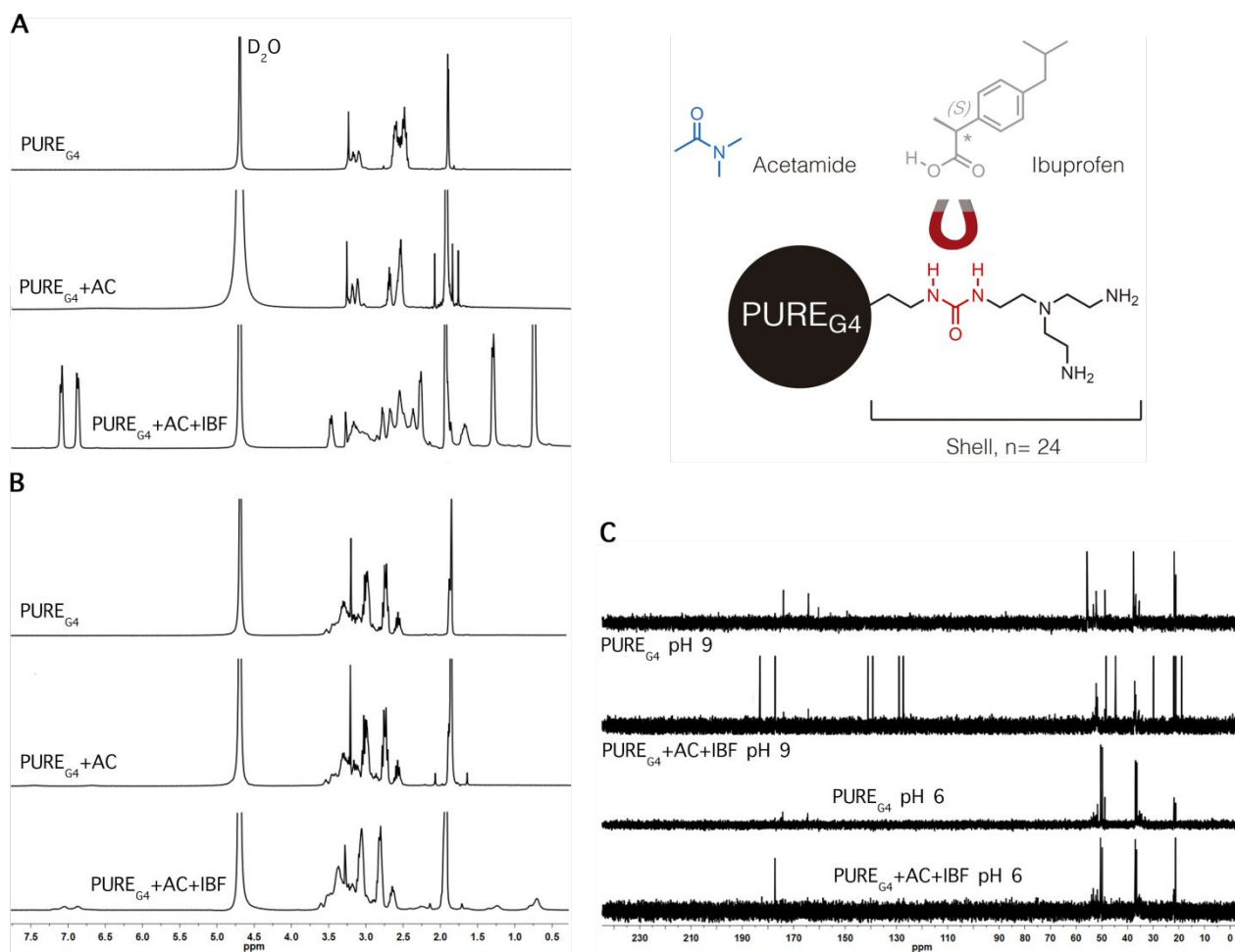


**Fig. 1** NMR spectra of PURE$_{G4}$ and PURE$_{G4}$ mixtures with acetamide (AC) (1:100) and ibuprofen (IBF) (1:37) at different pH values: $^1$H NMR spectra at pH 9 (A) and pH 6 (B), and $^{13}$C NMR spectra at pH 9 and 6. The figure shows the chemical structures of PURE$_{G4}$, AC and IBF. Strong hydrogen bonding between urea and carboxylic acid groups favors encapsulation of IBF into PURE$_{G4}$ biodendrimers.

Again, this preferential surface distribution may be due to the high penetration of water towards the core of the PURE biodendrimer (Fig. S4, ESI†) which may create a less favorable environment for IBF. To further characterize the interaction of acetamide molecules with PURE biodendrimers, two additional acetamide derivatives (*N,N*-diethyl and *N,N*-dimethyl acetamide), having a more hydrophobic character, were placed inside the dendrimer, one by one, up to a total of 20 molecules. Since acetamide has a high solubility in water this forces the interaction with PURE$_{G4}$ by preventing initial diffusion in the water box. However, like simulations of randomly placed ligands, acetamide molecules initially placed within the dendrimer rapidly diffused out of the dendrimer within the 5 ns of simulation (Fig. 3).
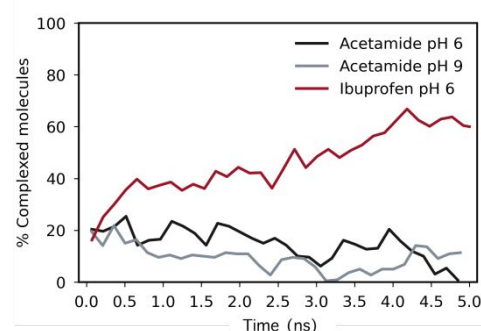


**Fig. 2** Distribution of acetamide (pH 6 and 9) and ibuprofen (pH 6) molecules in PURE biodendrimers. Molecules randomly placed in a water box that remain within 4 Å after 5 ns of simulations.
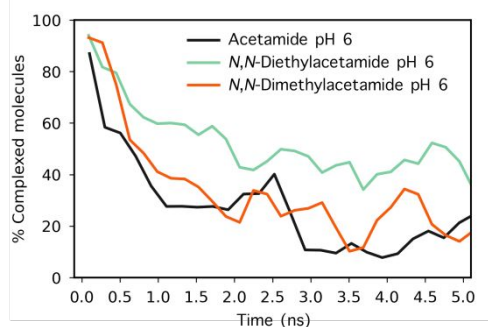
**Fig. 3** Distribution of acetamide, *N,N*-dimethylacetamide and *N,N*-diethyl acetamide molecules in PURE biodendrimers. Molecules initially placed inside PURE$_{G4}$ at pH 6 and simulated for 5 ns.

Only approximately 20% of acetamide molecules were found within 4 Å of the dendrimer after this timepoint which reiterates the absence of favorable interactions between acetamide and PURE biodendrimers. Interestingly, *N,N*-diethyl acetamide showed an increased retention within the dendrimer with slower diffusion out of the dendrimer in comparison to acetamide. In fact, 40% of the molecules remained within the dendrimer after the simulation time. Overall, the results indicate that inner hydrophobicity may be an important factor for successful encapsulation of guest molecules, which in agreement with previous observations for PAMAM dendrimers.

For both MD simulations, with free and docked guest molecules, the interactions are predominantly formed between the acetamide the carbonyl and the urea groups of the PURE biodendrimer, where hydrogen bonding enables formation of a *pseudo* 6-membered chelate ring. This agrees with reported strong interactions of acetamide with urea-containing molecules [23] or dimethylformamide [24] *via* bifurcated hydrogen bonding. Despite this interaction may be established, our *in vitro* and *in silico* data show a week interaction with PURE biodendrimer, which carry multiple urea groups. This weak interaction may be due to the open structure of the PURE biodendrimer that allows water to compete for the hydrogen bonding but also due to the flexibility of the dendrimer that may prevent a stable chelation. In fact, the potential role of water in hindering the complexation aligns with observations for polyglycine polymers, which interact with acetamide in dioxane but not in water [25]. Moreover, contrary to other macromolecules that form crystal structures with acetamide, the rapid shift of conformations that dendrimers undergo prevents a "pre-organization" for molecular binding of acetamide.

Since the presence of hydrophobic moieties seem to play an important role and as IBF is not soluble in water, we further evaluated the PURE biodendrimers nanofiltration capacity for water-soluble small molecules using MD simulations. In this regard, we had previously observed that PURE$_{G4-G6}$ biodendrimers at pH 7 interfered with the fluorescent readings of 5(6)-carboxyfluorescein (data not shown). This effect was concentration- and generation-dependent and was probably driven by aggregation of carboxyfluorescein molecules at the surface of PURE biodendrimers. Moreover, these complexes were stable even after addition of Triton X-100. To validate the aggregation mechanism, we carried out MD simulation of PURE$_{G4}$, PURE$_{G5}$ and PURE$_{G6}$ biodendrimers with 100 molecules of 5-carboxyfluorescein. Like PURE$_{G4}$, both PURE$_{G5}$ and PURE$_{G6}$ adopt a spherical conformation (Table 1) but have exponentially higher surface area and thus can establish more interactions at the surface. As it can be observed in Fig. 4, the results of interaction with 5-

carboxyfluorescein qualitatively correlate with the observations of aggregation at the surface and induced self-quenching *in vitro*. Like IBF, carboxyfluorescein molecules are located at the surface, thus forming a shell. Other dyes even with similar structure to fluorescein have been shown to interact with dendrimers at the surface/interior through interactions of amines with carboxyl groups [19,26,27].
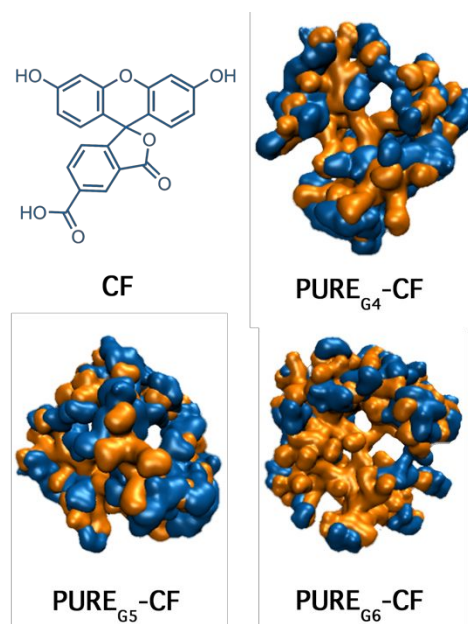


**Fig. 4** Snapshot of the surface area of different PURE biodendrimers generations (orange) and 5-carboxylfuorescein (CF, blue) after MD simulation.

Overall, our data is in good agreement with the observed fluorescence intensity drop observed in vitro as well as for other dyes interactions with PAMAM dendrimers. Moreover, both IBF and carboxyfluorescein show similar binding modes. A key aspect of dendrimer host-guest interactions is the location of the complexation. For acetamide, IBF and carboxyfluorescein both *in vitro* and *in silico* results suggest that these interactions are mostly at the surface. Moreover, these interactions appear to be driven by hydrogen bonding, electrostatic and hydrophobic interactions. Therefore, PURE biodendrimers in water were able to bind small molecules that are both soluble and insoluble in water and are more likely to bind to these than acetamide. This remarkable property is also of great advantage for nanofiltration purposes, especially when acetamide is a target contaminant, a strategy that could be integrated with membrane filtration systems [10].

## Experimental

### Materials

Acetamide (99% purity), *(S)*-(+)-ibuprofen (99%), tris(2-aminoethyl)amine (TREN, 96%) and *N,O*-bis(trimethylsilyl)acetamide (BSA, >95%) were purchased from Sigma Aldrich. Carbon dioxide was obtained from Air Liquide with a purity higher than 99.998%. All other chemicals were of analytical grade and used without further purification.

### Synthesis of PURE biodendrimers

**Journal Name**

**ARTICLE**

Generation 4 PURE biodendrimers ($PURE_{G4}$) were synthesized divergently following our methodology using a supercritical carbon dioxide ($scCO_2$)-assisted polymerization [12]. Briefly, TREN in the presence of BSA was reacted with $CO_2$ under supercritical conditions in a stainless-steel high-pressure cell. After depressurization more BSA and TREN were added and the mixture was heated to 120 °C leading to the first generation. Repetition of this process was carried to afford the fourth generation as a brownish viscous oil which was further purified by dialysis. Characterization and purity assessment were carried out by ^{1}H and ^{13}C NMR spectroscopy using a Bruker ARX 400 MHz spectrometer.

**PURE nanoformulations**

$PURE_{G4}$ biodendrimers nanoformulations were prepared using acetamide alone at a molar ratio of 1:100, 1:200 and 1:1000, or acetamide (1:100) in a crude mixture with IBF (1:37), in deuterated water at pH 6 and 9 at room temperature for 24 hours. The resulting nanoformulations were analyzed by ^{1}H and ^{13}C NMR spectroscopy.

**Molecular Dynamics Simulations**

All-atom PURE biodendrimers models of different generations ($PURE_{G4}$ to $PURE_{G6}$) were generated using a previously described method [17,18]. Monomers parameters for dendrimers assembly and for small molecules were obtained from *ParamChem* [28] based on the transferability of CHARMM General Force Field (CGenFF) [29]. Dendrimers were assembled from their monomer sequence and initial 3D structures were generated using *XPLOR v3.4* via a series of simulated annealing protocols using approach developed previously [17]. PURE biodendrimers with different protonation states were generated based on previously obtained titration curves [30]. For neutral pH only primary amines were protonated whereas for basic pH both primary and tertiary amines were modeled in their non-protonated state. Generated dendrimers were then immersed in a TIP3P water box model using the "solvate" module in *VMD v.1.9.1.* followed by the addition of ions to neutralize the charge using the "autoionize" module of VMD. Production runs were carried out in *NAMD v.2.9* [31] at 310 K using Langevin thermostat with a coupling constant of 5 ps$^{-1}$ and the integration time step of 2 fs. The SHAKE algorithm was used, and electrostatics were evaluated using the smooth particle mesh Ewald method with a Van der Waals cutoff of 12 Å. The system was then simulated in NPT conditions under periodic boundary conditions using NAMD for 5-35 ns. Additionally, Desmond employing OPLS-2005 forcefield and SPC water model was used to conduct simulated annealing simulations (SA) and molecular dynamics (MD) simulations for 3.13 ns and 10 ns, respectively. System builder implemented in *Maestro* as graphical user interface was used to immerse dendrimer in the SPC water box 10 Å larger than dendrimer in all directions. The SA calculations were setup to heat the system to 1000 K followed by cooling and further simulation at 300 K to overcome constraints due to arbitrary starting positions and were carried out using NVT and periodic boundary conditions. Last frame of SA trajectory was used as a starting point for MD simulation conducted under NPT conditions and using default values setup in *Maestro*. Simulations for different dendrimers were also performed in the presence of IBP (model API), acetamide (genotoxic impurity) and 5-carboxyfluorescein (water-soluble small molecule). These were either randomly distributed within a spherical shell of width comparable to one dendrimer's radius of gyration ($R_g$) around its periphery or by directly docking each molecule one after the other using *Autodock Vina*. All produced trajectories were analyzed in VMD. Analysis of obtained trajectories included the calculation of radius of gyration, root-mean-square deviation (RMSD), radial distribution of atoms and sphericity.[15] All obtained readouts were plotted using *matplotlib* and *seaborn plotting* packages in *Python 3.6*, handled within a *Jupyter Notebook*. The $R_g$ plots *versus* time reveal stable behavior for the last 20 ns that is indicative of adequate system equilibration. Thus, all obtained readouts, if required, were averaged over the interval of the last 20 ns for analysis.

## Conclusions

In the present work we disclosed the intrinsic ability of PURE biodendrimers to expel acetamide, a genotoxic impurity, and evaluated its potential as a nanofiltration system for purification and nanotherapeutic purposes. The formation of host-guest interactions is a complex process that is promoted by interactions with the solvent via electrostatic and hydrophobic interactions as well as hydrogen bonding. Examination of the dynamic properties of PURE biodendrimers revealed the distinct mode of binding of IBF and carboxyfluorescein compared to that of acetamide. At both neutral and basic conditions, acetamide interacts poorly with PURE biodendrimers. Moreover, MD simulations showed that even though small molecules bind mostly at the surface this still can translate into high drug payloads due to aggregation and these results were in qualitative agreement with *in vitro* experiments. Since PURE biodendrimers are biocompatible, non-cytotoxic and non-hemolytic polymers that can be synthesized using a green methodology in large scale and at low cost, its use as pharmaceutical excipients is of high potential for a combined strategy of acetamide removal and development of safe drug nanoformulations. Additionally, these bionanomaterials are also envisaged as effective nanofiltration enhancers.

## Conflicts of interest

There are no conflicts to declare.

## Acknowledgements

## References

This journal is © The Royal Society of Chemistry 20xx

*J. Mat. Chem. B*, 2021, **00**, 1-3 | **5**

1   G. Székely, J. Bandarra, W. Heggie, B. Sellergren and F. C. Ferreira, *J. Memb. Sci.,* 2011, **381**, 21.
2   A. Schülé, C. Ates, M. Palacio, J. Stofferis, J.-P. Delatinne, B. Martin and S. Lloyd, *Org. Process. Res. Dev.,* 2010, **14**, 1008.
3   R. Viveiros, V. D. B. Bonifácio, W. Heggie and T. Casimiro, *ACS Sustain. Chem. Eng.,* 2019, **7**, 15445.
4   P. Kolhe, E. Misra, R. M. Kannan, S. Kannan and M. Lieh-Lai, *Int. J. Pharm.*, 2003, **259**, 143.
5   I. Tanis and K. Karatasos, *J. Phys. Chem. B.,* 2009, **113**, 10984.
6   O. M. Milhem, C. Myles, N. B. McKeown, D. Attwood and A. D'Emanuele, *Int. J. Pharm.,* 2000, **197**, 239.
7   L. D. Pedro-Hernández, E. Martínez-Klimova, S. Cortez-Maya, S. Mendoza-Cardozo, T. Ramírez-Ápan and M. Martínez-García, *Nanomaterials (Basel),* 2017, **7**, 163.
8   P. Kolhe, J. Khandare, O. Pillai, S. Kannan, M. Lieh-Lai and R. M. Kannan, *Biomaterials,* 2006, **27**, 660.
9   A. Santos, F. Veiga and A. Figueiras, *Materials (Basel),* 2019, **13**, 65.
10  M. S. Diallo, Water treatment by dendrimer-enhanced filtration: Principles and applications *in* Nanotechnology applications for clean water – Solutions for improving water quality, A. Street, J. Duncan, R. Sustich, N. Savage (Eds.), 2014, 227.
11  M. Arkas, D. Tsiourvas and C. M. Paleos, *Chem. Mater.,* 2003, **15**, 2844.
12  R. B. Restani, P. I.  Morgado, M. P. Ribeiro, I. J. Correia, A. Aguiar-Ricardo and V. D. B. Bonifácio, *Angew. Chem. Int. Ed.,* 2012, **51**, 5162.
13  N. Martinho, H. Florindo, L. Silva, S. Brocchini, M. Zloh and T. Barata, *Molecules,* 2014, **19**, 20424.
14  R. B. Restani, A. S. Silva, R. F. Pires, R. Cabral, I. J. Correia, T. Casimiro, V. D. B. Bonifácio and A. Aguiar-Ricardo, *Part. Part. Syst. Charact.,* 2016, **33**, 851.
15  A. S. Ertürk, M. U. Gürbüz and M. Tülü, *Marmara Pharm. J.,* 2017, **21**, 385.
16  A. J. Perisé-Barrios, E. Fuentes-Paniagua, J. Sánchez-Nieves, M. J. Serramía, E. Alonso, R. M. Reguera, R. Gómez, F. Javier de la Mata and M. A. Muñoz-Fernández, *Mol. Pharm.,* 2016, **13**, 3427.
17  N. Martinho, L. Silva, H. Florindo, S. Brocchini, T. Barata and M. Zloh, *J. Comput. Aided Mol. Des.,* 2017, **31**, 817.
18  N. Martinho, L. Silva, H. Florindo, S. Brocchini, M. Zloh and T. Barata, *Int. J. Nanomedicine,* 2017, **12**, 7053.
19  L. F. Barraza, M. Zuñiga, J. B. Alderete, E. M. Arbeloa and V. A. Jiménez, *J. Lumin.,* 2018, **199**, 258.
20  P. K. Maiti, T. Çağin, S. T. Lin, W. A. Goddard, *Macromolecules,* 2005, **38**, 979.
21  P. K. Maiti, T. Çağın, G. Wang and W. A. Goddard, *Macromolecules,* 2004, **37**, 6236.
22  R. S. DeFever and S. Sarupria, Phys. *Chem. Chem. Phys.,* 2015, **17**, 29548.
23  T. Camellin, M. Acta, B. Cryst and B. M. Craven, *Acta Cryst.,* 1974, **B30**, 974.
24  R. J. Marshall, J. McGuire, C. Wilson and R. S. Forgan, *Supramol. Chem.,* 2018, **30**, 124.
25  J. Rupley and M. Praissman, *J. Am. Chem. Soc.,* 1963, **85**, 3526.
26  Y. García, V. A. Jiménez and J. B. Alderete, *J. Lumin.,* 2020, **222**, 117182.
27  G. Teobaldi and F. Zerbetto, *J. Am. Chem. Soc.,* 2003, **125**, 7388.
28  K. Vanommeslaeghe and Jr. A. D. MacKerell, *J. Chem. Inf. Model.,* 2012, **52**, 3144.
29  K. Vanommeslaeghe, E. Hatcher, C. Acharya, S. Kundu, S. Zhong, J. Shim, E. Darian, O. Guvench, P. Lopes, I. Vorobyov and Jr. A. D. Mackerell, *J. Comput. Chem.,* 2010, **31**, 671.
30  R. B. Restani, J. Conde, P. V. Baptista, M. T. Cidade, A. M. Bragança, J. Morgado, I. J. Correia, A. Aguiar-Ricardo and V. D. B. Bonifácio, *RSC Adv.,* 2014, **4**, 54872.
31  J. C. Phillips, R. Braun, W. Wang, J. Gumbart, E. Tajkhorshid, E. Villa, C. Chipot, R. D. Skeel, K. Kalé and K. Schulten, *J. Comput. Chem.,* 2005, **26**, 1781.

# Supporting Information

## Intrinsic acetamide brush-off by polyurea biodendrimers

Nuno Martinho,*[a] Rita F. Pires,[a] Mire Zloh,[b,c] and Vasco D. B. Bonifácio*[a]

[a] iBB-Institute for Bioengineering and Biosciences, Instituto Superior Técnico, Universidade de Lisboa, Lisboa, Portugal.
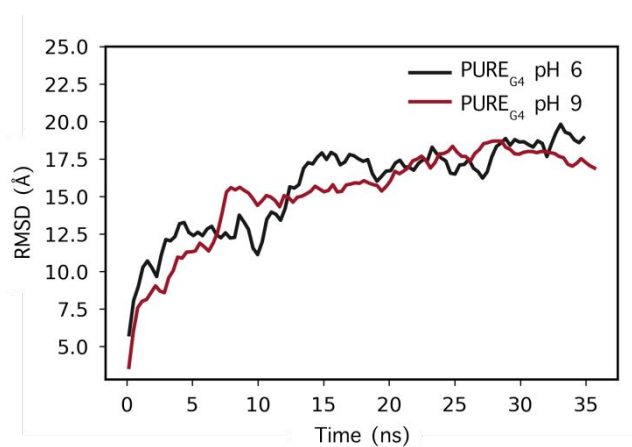[b] School of Life and Medical Sciences, University of Hertfordshire, Hatfield, United Kingdom.
[c] Faculty of Pharmacy, University Business Academy, Novi Sad, Serbia.

*E-mail: nunomartinho@tecnico.ulisboa.pt; vasco.bonifacio@tecnico.ulisboa.pt

**Fig. S1** Acetamide crystals that crystalized out of a $PURE_{G4}$ biodendrimer crude mixture.



**Fig. S2** Root mean square deviation of simulated $PURE_{G4}$ biodendrimers at different pH values. Equilibration was achieved after approximately 10 ns.
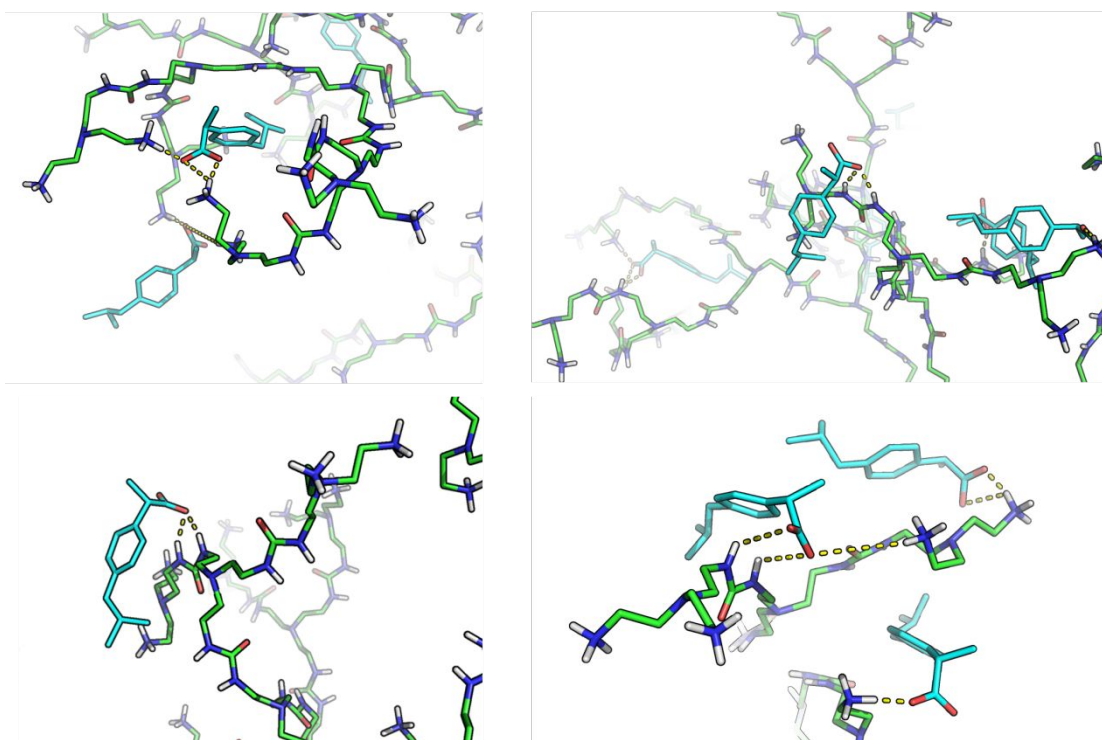
**Fig. S3** Interactions of ibuprofen with the $PURE_{G4}$ biodendrimer in the last snapshot. Several interactions are observed: terminal amines from multiple dendrimer branches with the carboxylic acid of ibuprofen, as well as bidentate bridges between the urea motif of $PURE_{G4}$ and the carboxylic acid of ibuprofen.
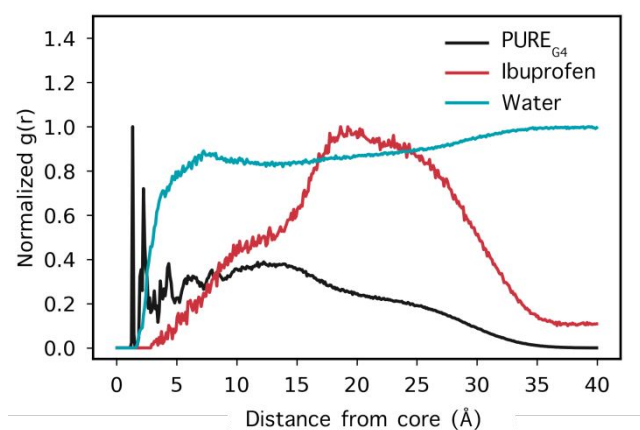


**Fig. S4** Radial distribution of dendrimer branches, ibuprofen, and water molecules from the core of a $PURE_{G4}$ biodendrimer. Ibuprofen is majorly distributed at the terminal branches while water has a high penetration into the interior.

# Table of Contents

Polyurea biodendrimers display an intrinsic affinity-repulsion fitness towards drug-acetamide mixtures, turning these nanocarriers an attractive platform for APIs purification and/or preparation of genotoxic-free nanoformulations.
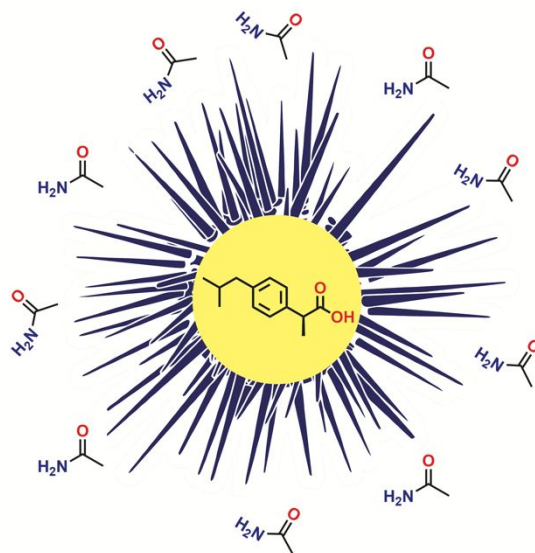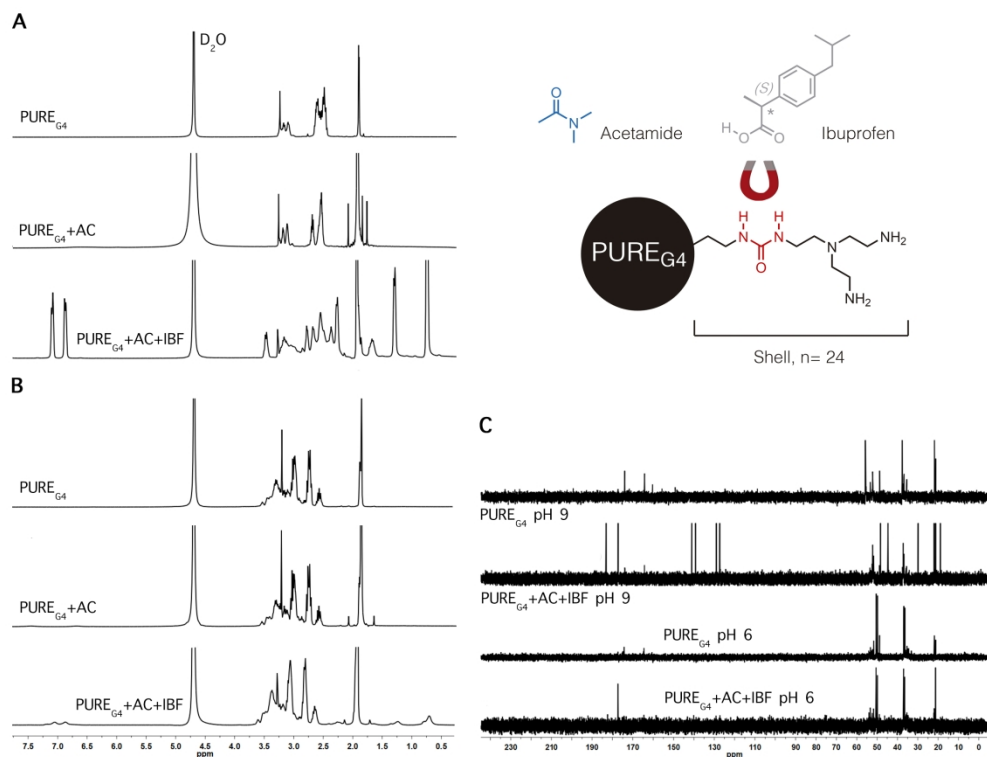
Fig. 1 NMR spectra of PURE$_{G4}$ and PURE$_{G4}$ mixtures with acetamide (AC) (1:100) and ibuprofen (IBF) (1:37) at different pH values: $^1$H NMR spectra at pH 9 (A) and pH 6 (B), and $^{13}$C NMR spectra at pH 9 and 6. The figure shows the chemical structures of PURE$_{G4}$, AC and IBF. Strong hydrogen bonding between urea and carboxylic acid groups favors encapsulation of IBF into PURE$_{G4}$ biodendrimers.
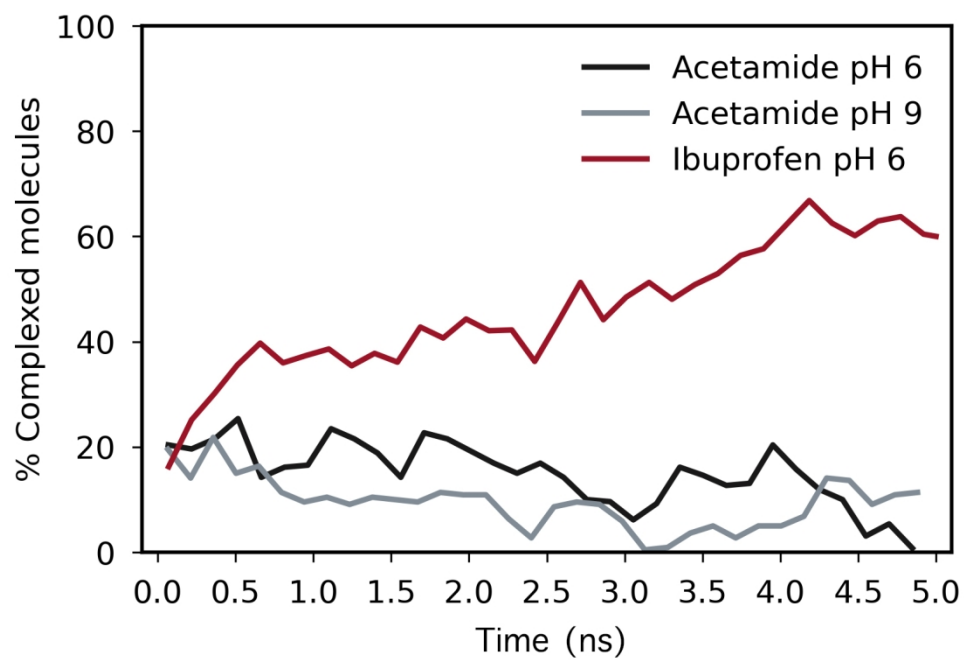
512x390mm (150 x 150 DPI)

Fig. 2 Distribution of acetamide (pH 6 and 9) and ibuprofen (pH 6) molecules in PURE biodendrimers. Molecules randomly placed in a water box that remain within 4 Å after 5 ns of simulations.
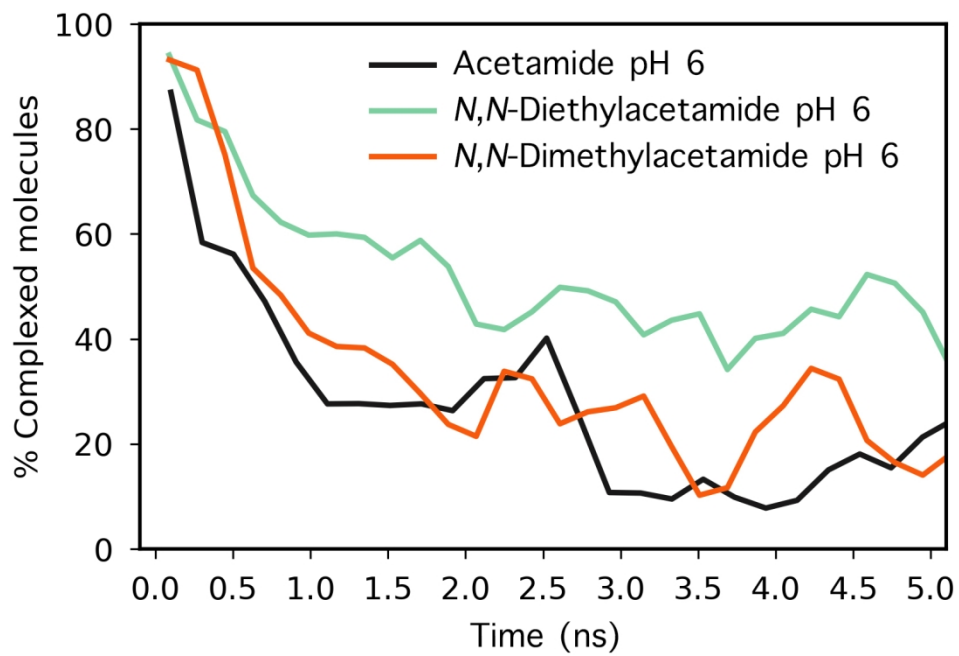
364x254mm (120 x 120 DPI)

Fig. 3 Distribution of acetamide, *N,N*-dimethylacetamide and *N,N*-diethyl acetamide molecules in PURE biodendrimers. Molecules initially placed inside PURE$_{G4}$ at pH 6 and simulated for 5 ns.
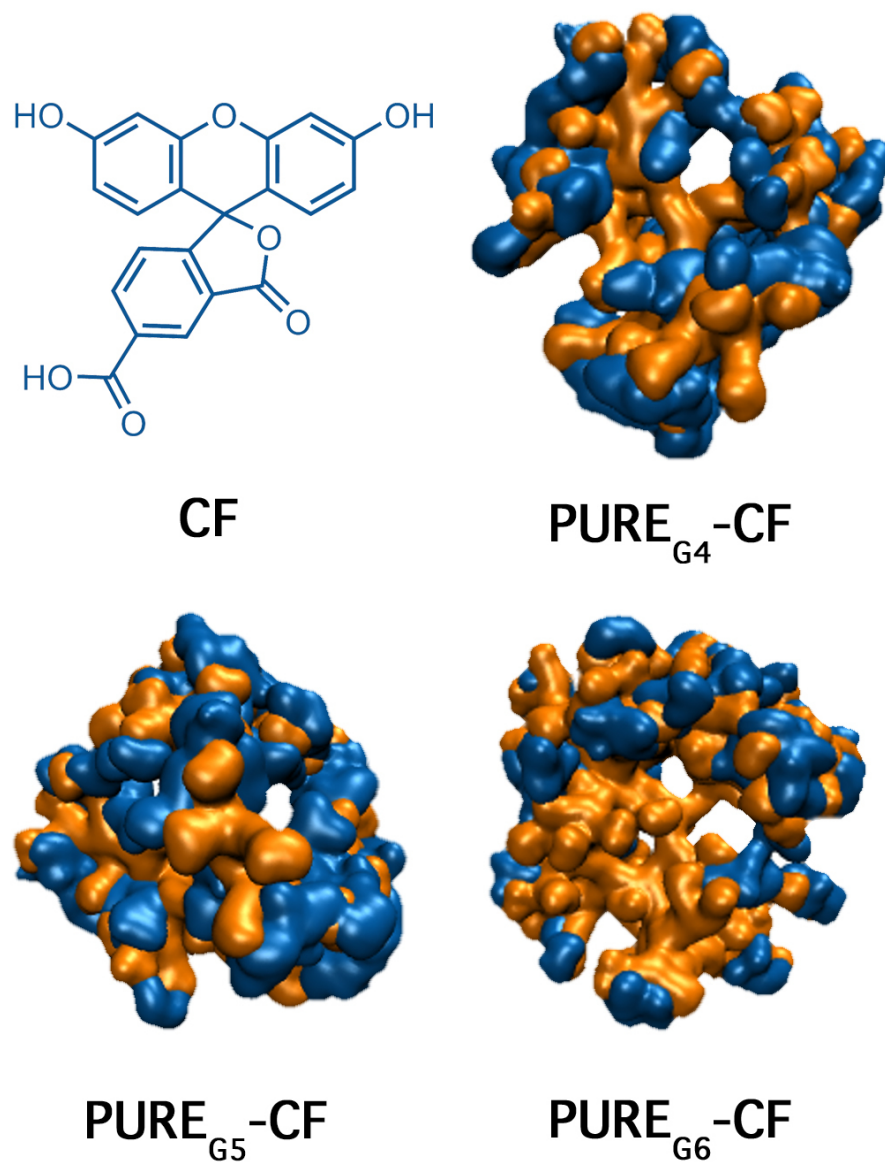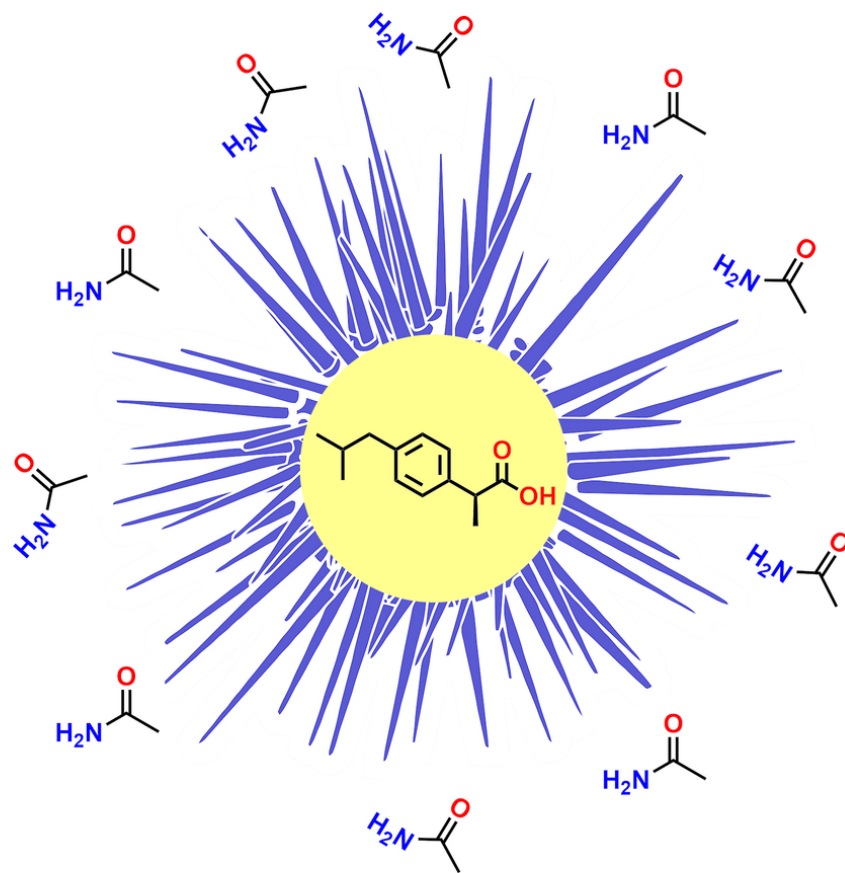
366x253mm (120 x 120 DPI)

Fig. 4 Snapshot of the surface area of different PURE biodendrimers generations (orange) and 5-carboxylfuorescein (CF, blue) after MD simulation.

180x229mm (150 x 150 DPI)

Graphical Abstract

83x83mm (300 x 300 DPI)